

3D MODELING OF FLOATING STRUCTURES FOR OFFSHORE WIND ENERGY: PRELIMINARY HYDROSTATIC BEHAVIOR AND TANK TESTING

Mariana T. de Moraes ¹; James Hall ²; Carina M. Stolz ³; Assed Haddad⁴; Alex Ximenes Naves⁵

¹Engenheira ambiental | marianat.moraes@poli.ufrj.br | PEA-UFRJ | Rio de Janeiro, Brasil; ²Doutor em Engenharia | Jameshall@id.uff.br | UFF | Niterói, Brasil; ³Doutora em Engenharia | carinastolz@poli.ufrj.br | PEA-UFRJ | Rio de Janeiro, Brasil; ⁴Doutor em Engenharia | assed@poli.ufrj.br | PEA-UFRJ | Rio de Janeiro, Brasil; ⁵Doutorando em Engenharia | axnaves@id.uff.br | PEA-UFRJ | Rio de Janeiro, Brasil;

Resumo:

Este estudo apresenta uma abordagem experimental para o desenvolvimento de flutuadores utilizados na geração de energia eólica offshore, com foco na modelagem 3D e em testes em tanque para avaliação hidrostática. Inspirado em pesquisas anteriores da Universidade de Edimburgo, o estudo propõe um processo iterativo de design e teste de protótipos impressos em PLA. Três diferentes modelos de flutuadores foram desenvolvidos e avaliados quanto à flutuabilidade, estabilidade e capacidade de suporte de carga associada a estruturas de turbinas eólicas. Os resultados mostraram que a geometria oca com volume aumentado apresentou desempenho superior em termos de flutuabilidade e estabilidade, conforme validado por meio de experimentos em tanque d'água. Esses achados ressaltam a relevância da combinação entre modelagem numérica e prototipagem física para aprimorar o projeto de estruturas flutuantes em ambientes offshore.

Palavras-chave:

Energia eólica; offshore; modelagem; protótipos; flutuadores.

Abstract:

This study presents an experimental approach for developing floaters used in offshore wind energy, focusing on 3D modeling and tank testing for hydrostatic assessment. The study is inspired by previous research from the University of Edinburgh and proposes an iterative process of designing and testing PLA-printed prototypes. Three different floater designs were developed and evaluated in terms of buoyancy, stability, and load-bearing capacity in relation to wind turbine structures. The results showed that the hollow geometry with increased volume demonstrated superior performance in terms of buoyancy and stability, as validated through water tank experiments. These findings highlight the relevance of combining numerical modeling and physical prototyping to improve the design of floating structures in offshore environments.

Keywords:

Wind Energy; offshore; Modeling; Prototypes; Floaters.

1. INTRODUCTION

It is widely recognized that the ocean is an important component of the climate system, playing a fundamental role in regulating global temperatures (Huybers, 2010). Given this critical influence, growing concerns about climate change have prompted countries to pursue alternative energy sources that minimize environmental impact. In this context, nuclear, solar, wind, geothermal, and biomass energy, along with efforts to improve energy efficiency, have gained increased global attention (Schrag, 2007). Among these, offshore wind energy has emerged as one of the most promising forms of clean and sustainable energy generation (Karimirad *et al.*, 2011). By harnessing stronger and more consistent winds over the ocean, offshore turbines can achieve significantly higher energy output.

This technology offers significant potential to meet the growing global energy demand sustainably. However, before deploying offshore wind farms on a large scale, it is essential to understand the dynamic behavior of floaters under real ocean conditions (Bilgen, Kaygusuz, Sari, 2010).

3D modeling plays a crucial role in the analysis and optimization of offshore wind structure performance (Mitarai, 2016). According to research conducted by the University of Edinburgh, "Hydrodynamic response of a stepped-spar floating wind turbine: Numerical modelling and tank testing", numerical modeling combined with water tank testing enables a detailed analysis of the hydrodynamic behavior of floaters, providing valuable insights for the design and operation of floating wind turbines (Sethuraman, Venugopal, 2021). This experimental approach makes it possible to study the behavior of structures in response to different wave and wind conditions, allowing for a better understanding of the challenges faced in the offshore environment.

Scientific communities focused on large-scale hydrological modeling have been seeking ways to represent, monitor, and predict these unexpected phenomena with greater temporal and spatial accuracy (Rougé *et al.*, 2021). In this context, this paper proposes the use of 3D modeling to develop a scaled-down structure of a floating offshore wind platform. The main objective is to study the hydrodynamic response of the platform based on three-dimensional modeling and experimental tests conducted in a wave tank, contributing to advances in the simulation of structural behavior under real ocean conditions.

2. LITERATURE REVIEW

In recent decades, offshore wind energy has gained prominence as a clean, abundant, and viable alternative to traditional energy sources (Gideon and Bou-Zeid, 2021). The possibility of installing wind turbines in the ocean allows for the harnessing of stronger and more consistent winds, with less interference from urban elements (Wieczorek *et al.*, 2013).

In this context, studies such as those by the European Wind Energy Association (EWEA, 2012) emphasize that offshore technology, by taking advantage of stronger and more consistent winds at sea, experiences fewer urban interferences, promoting high energy efficiency. Additionally, reports such as KPMG (2010) indicate that the expansion of this sector in Europe is directly linked to favorable public policies and technical innovations.

However, the development of technologies for floating turbines in offshore environments presents significant challenges in terms of stability, anchoring, and the dynamic behavior of structures subjected to severe maritime conditions. Therefore, several studies have focused on experimental and numerical modeling of the hydrodynamic behavior of these systems (He *et al.*, 2024). In this sense, the dynamic behavior of offshore platforms under wave and wind actions remains an unresolved and complex issue, and a challenge in engineering (Shang *et al.*, 2024).

Computational modeling with tools such as OrcaFlex, combined with physical prototyping and wave tank testing, has been widely used to predict the dynamic response of spar-type and semi-submersible platforms (Seebai and Sundaravadivelu, 2009; Utsunomiya *et al.*, 2009). However, the technological obstacles associated with highly compatible offshore designs challenge many existing

simulation techniques, as wind and wave forces are irregular and nonlinear (Wang and Sweetman, 2011).

Furthermore, approaches such as the use of vibration control systems, innovative structural configurations, and mooring line analyses have also been studied to mitigate structural risks (Jonkman et al., 2011).

These studies are necessary because the interaction between waves and offshore structures is bidirectional; the structure responds to hydrodynamic loads and alters the flow field around it. Additionally, offshore structures are exposed to higher waves than coastal structures, as well as a variety of different load scenarios, including short-crested wind waves combined with strong winds, longer swell waves, gusts, breaking waves, and intense currents (Tomasicchio *et al.*, 2018).

The experimental validation of scaled models is considered an essential step in the design process, allowing not only for the direct observation of the effects of waves and winds but also for the calibration of computational models (Goupee *et al.*, 2014). Studies such as those by Payne et al. (2008) reinforce the importance of comparing experimental results and numerical simulations for validating marine energy devices.

Thus, this study highlights that the integration of 3D modeling, reduced-scale experimentation, and numerical simulation represents a promising path to advance the development of offshore wind platforms, providing a more solid technical foundation for the design and operation of these structures in marine environments.

3. METHODOLOGY

The development of this article involved the design and prototyping of different floating platform models for offshore wind turbines, using 3D modeling tools, PLA printing, and buoyancy tests in a water tank. The methodology was divided into three main stages: computational modeling, material selection and printing preparation, 3D printing, and experimental testing, as shown in Figure 1.

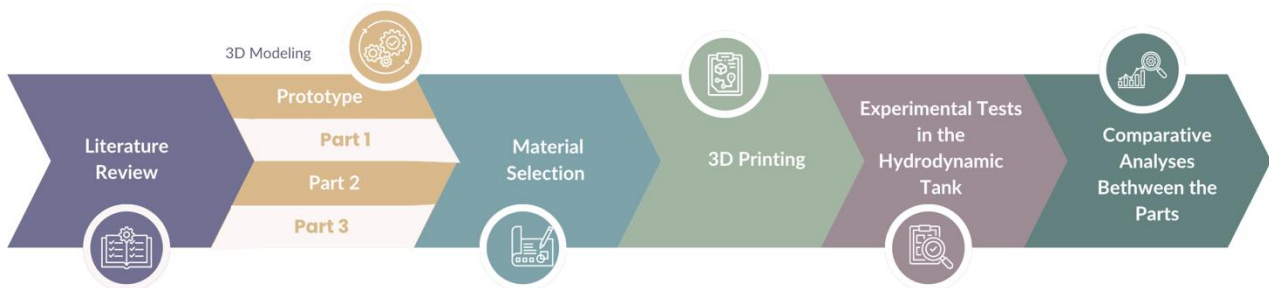


Figure 1: Flowchart.

3.1. 3D COMPUTATIONAL MODELING (ONSHAPE)

The parts were modeled using the Onshape platform, a cloud-based CAD software with parametric modeling and simulation capabilities. Three distinct versions of floaters were designed: an initial prototype, a hollow part (Part 1), a solid part (Part 2), and finally, a hollow part with increased volume (Part 3).

Each geometry was designed based on technical parameters aimed at optimizing the stability and buoyancy of the structures in offshore environments. Key criteria included internal volume, crucial for increasing buoyant force, the mass distribution to reduce overturning moments, and the ratio between base area and floater height, which influences hydrostatic stability. Wall thickness was also evaluated to balance structural strength and lightness, and the center of mass was lowered to enhance stability against wave and wind action.

3.2. MATERIAL SELECTION AND PREPARATION FOR 3D PRINTING

PLA (polylactic acid) was chosen as the printing material due to its mechanical strength, low moisture absorption, and suitability for rapid prototyping. In addition, it offers good impact resistance, stiffness, and dimensional stability. These properties are essential for withstanding harsh maritime conditions, including exposure to salt water, strong winds, and waves (Letcher et al., 2015).

Although PLA has a specific density between 1.24 and 1.27 g/cm³, higher than that of water (1 g/cm³ at 25°C), its properties can be adjusted for specific applications. Through the addition of expansion agents or the use of advanced design techniques, cavities or hollow spaces can be incorporated into the structure, decreasing the final density of the object and enabling it to float in water. This makes PLA a strategic choice for projects in marine environments (Letcher et al., 2015).

Moreover, PLA is notable for its flexibility in 3D printing, allowing the creation of prototypes with complex geometry and high precision. This technology enables detailed evaluation of both the design and physical properties of the material prior to industrial-scale production (Letcher et al., 2015). Thus, the files generated in Onshape were exported to FlashPrint 5, the software responsible for slicing and generating the code needed for the GTMAX3D Core H4 3D printer. Parameters such as filament density, print speed, and wall thickness were adjusted according to the specifications of each part.

3.3. 3D PRINTING OF PROTOTYPES

The 3D printing process was carried out in the Prototyping Laboratory of the Fluminense Federal University. The average print time ranged from 1h15 to 2h07, depending on the complexity and volume of each piece. After printing, the parts were joined using high-strength adhesive (Super Bonder), ensuring proper sealing and structural integrity for the flotation tests.

3.4. FLOTATION TESTS IN EXPERIMENTAL TANK

The printed parts underwent flotation tests in a water tank filled with salt water to approximate marine conditions. Although the tank included features such as stones to represent seabed irregularities and a wave generator, no dynamic effects were measured; the tests were limited to hydrostatic analysis focused on stable flotation and buoyancy. The buoyant force was calculated based on the displaced fluid volume, according to Equation 1.

$$B = \rho_{\text{water}} \cdot V \cdot g \text{ (Eq. 1)}$$

$$\rho_{\text{water}} = 1000 \text{ kg/m}^3;$$

$$g = 9,81 \text{ m/s}^2;$$

V = submerged volume of the part;

Additionally, it was necessary to convert the kilograms into Newtons in order to compare it with the estimated weight, using the following Equation 2.

$$W = m \cdot g \text{ (Eq. 2)}$$

W = weight (in Newtons),

m = mass (in kilograms),

g = acceleration due to gravity (9.81 m/s²).

The efficiency of each model was evaluated based on its ability to support not only its own weight but also the estimated mass of the wind turbine structure. A minimum requirement was established: the models should support at least twice its own mass. This safety factor of 2 was adopted based on preliminary estimates of the additional load from the turbine components, such as the tower, rotor, generator, and connecting elements, and was intended to ensure operational stability under simulated offshore conditions. The use of this threshold allowed the team to eliminate inadequate designs early in the testing phase while still enabling iterative improvements to the more promising prototypes.

4. RESULTS AND DISCUSSION

The results obtained from the development of four different floater models, initial prototype, Part 1 (hollow), Part 2 (solid), and Part 3 (hollow with increased volume), were analyzed individually. Each part was evaluated based on its dimensions, mass, displaced volume, buoyancy, and performance in experimental tests to identify the most viable alternative for offshore wind turbine applications.

4.1. INITIAL PROTOTYPE

The initial prototype aimed to assess the feasibility of the modeling, printing, and basic flotation process using PLA. With a cylindrical geometry and a mass of 0.047 kg, the prototype had a volume of 0.00004463 m³. This results in an apparent density of approximately 1053 kg/m³. This lower-than-expected value compared to solid PLA (1.24–1.27 g/cm³) is due to the inclusion of internal air cavities during the printing process, which reduced the overall density and allowed the prototype to float. The buoyancy was calculated based on Eq. 1, where:

$$B = 1000 \times 0.00004463 \times 9.8 \approx 0.437 \text{ N}$$

The prototype's weight, calculated as:

$$W = m \cdot g = 0.047 \cdot 9.81 \approx 0.461 \text{ N}$$

Comparison shows that the buoyant force (0.437 N) was slightly lower than the prototype's weight (0.461 N), which aligns with experimental observations of near-neutral but stable flotation, with the part partially submerged and remaining horizontally oriented during testing (Figures 2a and 2b). Despite not being designed to support external loads, the prototype served to validate the printing method and material selection under laboratory conditions.

The observed flotation behavior confirmed that the internal cavities were effective in reducing density, and the tank test validated the feasibility of using PLA in hydrostatic applications when combined with suitable geometric adjustments.



Figures 2a and 2b - Buoyancy test of the prototype in the laboratory tank.

4.2. PART 1 – HOLLOW FLOATER

Part 1 maintained the geometry of the prototype but incorporated modifications to allow anchoring (lateral flaps) and better fitting of the wind turbine tower, as shown in Figure 3.

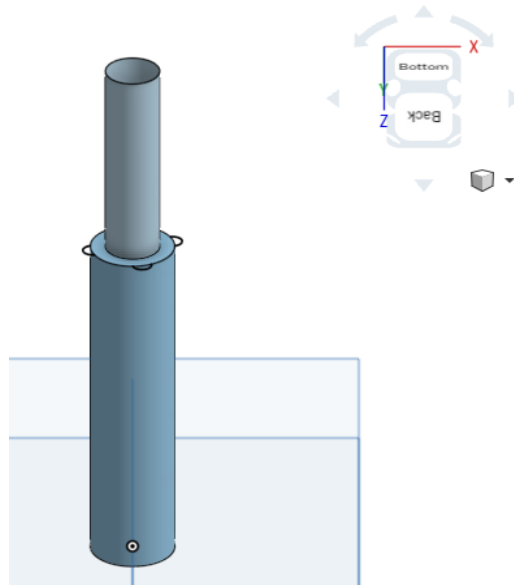


Figure 3 - 3D modeling of Part 1 (front view).

Although the design allowed for a more functional assembly, the buoyancy calculations revealed a critical limitation:

- **Total displaced volume:** 0.00004463 m^3 (larger cylinder) + 0.000003738 m^3 (smaller cylinder);
- **Estimated buoyancy:** $B = 1000 \times 0.00004837 \times 9.8 \approx 0.474 \text{ N}$;
- **Weight of the part:** $W = 0.051 \times 9.81 \approx 0.500 \text{ N}$ $NW = 0.051 \times 9.81 \approx 0.500 \text{ N}$;

The part presented buoyancy lower than its own weight, resulting in negative flotation. This indicates that, even without additional load, the structure would sink. This outcome reflects the limitation of the internal volume in the original hollow geometry and highlights the need for changes in mass distribution or total volume. Since it did not meet the requirement of supporting at least twice its own weight, Part 1 was discarded.

4.3. PART 2 – SOLID FLOATING DEVICE

Part 2 maintained the external geometry of Part 1, but with a solid fill. This modification aimed to increase mass and, indirectly, stability. However, the calculations revealed another limitation.

- **Total displaced volume:** 0.00007389 m^3 (larger cylinder) + 0.000003738 m^3 (smaller cylinder);
- **Estimated buoyancy:** $B = 1000.0 \times 0.00007763.9 \times 8 \approx 0.761 \text{ N}$;
- **Weight of the part:** $W = 0.081 \times 9.81 \approx 0.794 \text{ N}$ $NW = 0.081 \times 9.81 \approx 0.794 \text{ N}$;

Even with a slightly larger volume than Part 1, the increase in mass compromised buoyancy. The part also exhibited negative buoyancy, being unable to support even its own weight. This result reinforces that increasing density (solid fill) compromises buoyancy and the part's function as a floating device. Part 2 was also discarded.

4.4. PART 3 – HOLLOW FLOATING DEVICE WITH INCREASED VOLUME

Part 3 was designed with significant modifications: larger diameter and height, thinner walls, and increased volume. The goal was to achieve enough buoyancy to support the mass of the part and the turbine structure.

- **Total displaced volume:** 0.0002045 m^3 (larger cylinder) + 0.000003738 m^3 (smaller cylinder);
- **Estimated buoyancy:** $B = 1000.0 \times 0.0002082 \times 9.8 \approx 2.04 \text{ N}$;

- **Weight of the part:**
- Upper section (0.004 kg) + Lower section (0.019 kg) = 0.023 kg →
 $W=0.023 \times 9.81 \approx 0.226 \text{ N}$;
- **Remaining load capacity:**
- $2.04 \text{ N} - 0.226 \text{ N} \approx 1.814 \text{ N}$;

Part 3 demonstrated excellent performance and was printed, as shown in Figures 4a and 4b.



Figure 4a and 4b - Part 3 near the laboratory tank.

Its buoyancy was about nine times greater than the weight of the structure, providing safety for supporting the scaled-down wind turbine tower. The practical test in the tank confirmed the stability and positive buoyancy of the structure, as shown in Figure 5. The possibility of adding mass to the base further improves stability, making this model the most promising among those evaluated.



Figure 5 - Buoyancy test of Part 3 in the laboratory tank.

Due to the dimensions and complexity of Part 3's geometry, the 3D printing was carried out in two distinct stages to ensure dimensional accuracy, better process control, and optimal use of the laboratory resources.

In the first stage, the upper part of the structure was printed, which includes the smaller cylinder (for the wind turbine tower fitting) and the piece's cap. This printing took approximately 1 hour and 15

minutes. This part was precisely designed to allow a direct fit into the lower part of the structure, as shown in Figure 6.



Figure 6 - 3D modeling of Part 3 (front view of the cap).

In the second stage, the lower part was printed, consisting of the larger cylinder and the side flanges responsible for securing the float, as shown in Figure 7. This stage took about 2 hours and 7 minutes, due to the larger volume and thickness of the outer walls, which were necessary to ensure structural strength and stability in the water.

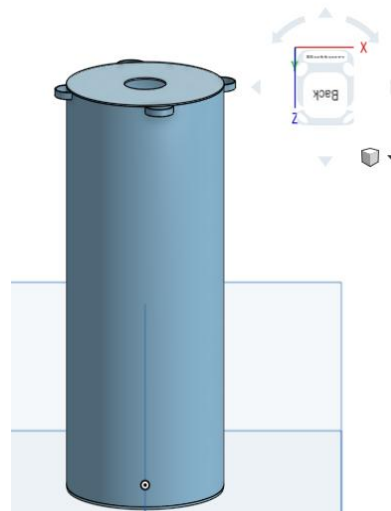


Figure 7 – 3D modeling of Part 3 (front view of the larger cylinder).

After the parts cooled down, the two sections were joined using high-strength instant glue (Super Bonder). The bonding process was conducted manually to ensure the correct fit of the surfaces and prevent leaks. The sealing between the parts was crucial to preserve the internal air volume and, consequently, the buoyancy of the system.

The success of the final assembly was confirmed through tank tests, in which the part maintained its structural integrity, showed no leakage, and withstood mechanical variations simulated by forces applied by the researchers. These variations were generated by the wave maker system, which produced waves of constant intensity, and by the action of a fan operating at maximum power, simulating gusts of wind striking the structure. The glued joint between the parts withstood well in contact with the water, validating the connection method used for small-scale prototypes.

After the parts cooled down, the two sections were joined using high-strength instant glue (Super Bonder). The bonding process was carried out manually to ensure the correct fit of the surfaces and prevent leaks. The sealing between the parts was crucial to preserve the internal air volume and, consequently, the buoyancy of the system.

The success of the final assembly was confirmed through tank tests, in which the part maintained its structural integrity, showed no leakage, and withstood simple mechanical disturbances applied by the researchers. These disturbances were not measured quantitatively, and no hydrodynamic data were collected. The wave maker system produced constant low-amplitude waves, and a fan operating at maximum power was used to simulate the visual effect of wind impact, both serving to test the prototype's structural behavior qualitatively. The glued joint between the parts remained intact and watertight, validating the connection method used for small-scale prototypes.

4.5. COMPARISON BETWEEN THE PARTS

The analysis of the three parts developed highlights the importance of correctly sizing the volume and mass to ensure the hydrodynamic efficiency of floating devices in offshore wind turbines. Therefore, a comparative analysis between the models is necessary, as shown in Table 1:

Parameter	Initial Prototype	Part 1 (Hollow)	Part 2 (Solid)	Part 3 (Hollow with Increased Volume)
Buoyancy (N)	0,437	0,474	0,761	2,04
Weight (N)	0,461	0,500	0,794	0,226
Additional Mass Supported (N)	-0,0025	-0,0026	-0,0033	+0,185
Observed Buoyancy	Stable	Sinks	Sinks	Stable and Positive
Feasibility for Wind Turbine	Low (no load)	None	None	High (with safety margin)

Table 1: Comparison between parts.

Part 1, although designed with a functional design for anchoring and integration with the tower, had insufficient volume to generate buoyancy capable of supporting its weight. The attempt to create internal cavities as a buoyancy strategy was limited by the narrow geometry and the fixed proportions of the design.

Part 2, conceived as a solid version of Part 1, significantly increased the mass without expanding the displacement volume. The result was even more unsatisfactory in terms of buoyancy, since the increased density caused the total weight to exceed the available buoyant force, leading to negative flotation. This experiment clearly demonstrated that increasing density directly compromises flotation performance, even when the external geometry remains constant.

In contrast, Part 3 successfully incorporated the necessary corrections: an increase in total volume, reduction of structural mass through thin internal walls, and separation into modules to facilitate printing and assembly. The buoyancy achieved was sufficient not only to keep the structure stably afloat but also to support an estimated additional load equivalent to the scaled wind turbine components. The decision to print the part in separate sections allowed overcoming the limitations of the 3D printer while ensuring precision in assembly and watertight sealing.

Finally, the study demonstrated that the integration of computational modeling, 3D printing, and experimental validation provides an efficient and low-cost pathway for the development and preliminary evaluation of floating structures for offshore applications.

5. CONCLUSION

This article demonstrated the feasibility and importance of 3D modeling combined with rapid prototyping in the design of floaters for offshore wind turbines. In this way, it was possible to evaluate, compare, and improve different geometries and part configurations based on criteria of stability, buoyancy, and mass.

The use of PLA as the material for 3D printing proved to be suitable for small-scale testing, ensuring structural rigidity, dimensional accuracy, and adequate performance in controlled hydrostatic environments.

Part 3, the result of accumulated improvements between the test parts, showed significantly superior performance in terms of buoyancy, stability, and the ability to support additional load. The model was printed in parts, successfully assembled, and subjected to flotation tests in a laboratory tank, validating its potential as a functional base for future applications in floating turbines and reinforcing the importance of geometric and mass distribution adjustments for hydrostatic equilibrium.

Therefore, this study contributes to the advancement of knowledge in offshore wind energy, not only by presenting a technical prototyping methodology but also by emphasizing the importance of practical experimentation in applied engineering projects, particularly in the early validation of floating support structures.

6. REFERENCES

BILGEN, S.; KAYGUSUZ, K.; SARI, A. Renewable energy for a clean and sustainable future. **Energy Sources, Part B: Economics, Planning, and Policy**, v. 5, n. 2, p. 1119–1129, 2010. Available at: <https://doi.org/10.1080/00908310490441421>

CHAN, D.; GEBBIE, G.; HUYBERS, P. An improved ensemble of land surface air temperatures since 1880 using revised pair-wise homogenization algorithms accounting for autocorrelation. **Journal of Climate**, online publication: 12 Mar. 2024; print: 1 Apr. 2024. <https://doi.org/10.1175/JCLI-D-23-0338.1>

EUROPEAN WIND ENERGY ASSOCIATION. **The European offshore wind industry key 2011 trends and statistics**. January 2012. Available at: http://www.ewea.org/fileadmin/ewea_documents/documents/publications/statistics/EWEA_stats_of_fshore_2011_01.pdf

EUROPEAN WIND ENERGY ASSOCIATION. **Wind in power: 2012 European statistics**. February 2012. Available at: [https://www.ewea.org/fileadmin/files/library/publications/statistics/Wind in power annual statistics_2012.pdf](https://www.ewea.org/fileadmin/files/library/publications/statistics/Wind_in_power_annual_statistics_2012.pdf)

GIDEON, R. A.; BOU-ZEID, E. Collocating offshore wind and wave generators to reduce power output variability: A multi-site analysis. **Renewable Energy**, v. 163, p. 1548–1559, Jan. 2021. Available at: <https://doi.org/10.1016/j.renene.2020.10.102>

HE, Y. *et al.* Hydrodynamic modulation instability triggered by a two-wave system. **Chaos (AIP Publishing)**, v. 34, 103108, 2024. Available at: <https://doi.org/10.1063/5.0220359>

JONKMAN, J. M.; ROBERTSON, A. N. Loads analysis of several offshore floating wind turbine concepts. In: **Proceedings of the 21st International Offshore and Polar Engineering Conference**, Maui, Hawaii, 2011. Available at: <https://onepetro.org/ISOPEIOPEC/proceedings-abstract/ISOPE11/All-ISOPE11/13294>

KARIMIRAD, M.; MEISSONNIER, Q.; GAO, Z.; MOAN, T. Hydro-elastic code-to-code comparison for a tension leg SPAR-type floating wind turbine. **Marine Structures**, v. 24, n. 4, p. 412–435, 2011. Available at: <https://doi.org/10.1016/j.marstruc.2011.05.006>

KPMG. **Market report:** Offshore wind in Europe. 2010. Available at: http://www.kpmg.com/UK/en/IssuesAndInsights/ArticlesPublications/Documents/PDF/Market%20Sector/Power_and_Utillities/KPMG_Offshore_Wind_in_Europe_eng_FINAL.pdf

LETCHER, T.; WAYTASHEK, M. Material property testing of 3D-printed specimen in PLA on an entry-level 3D printer. In: **ASME - International Mechanical Engineering Congress and Exposition (IMECE)**, Brookings, SD, 2014. Paper No: IMECE2014-39379, V02AT02A014, 8 p. Available at: <https://doi.org/10.1115/IMECE2014-39379>

MITARAI, S. *et al.* Quantifying dispersal from hydrothermal vent fields in the western Pacific Ocean. **PNAS**, v. 113, n. 11, p. 2976–2981, 2016. Available at: <https://doi.org/10.1073/pnas.1518395113>

PAYNE, G. S. *et al.* Assessment of boundary-element method for modelling a free-floating sloped wave energy device. Part 2: Experimental validation. **Ocean Engineering**, v. 35, p. 342–357, 2008. Available at: <https://doi.org/10.1016/j.oceaneng.2007.10.008>

ROUGÉ, C. *et al.* Coordination and control – limits in standard representations of multi-reservoir operations in hydrological modeling. **Hydrology and Earth System Sciences**, v. 25, p. 1365–1382, 2021. Available at: <https://doi.org/10.5194/hess-25-1365-2021>

SHANG, B. *et al.* Detailed nonlinear modeling and high-fidelity parallel simulation of MMC with embedded energy storage for wind farm grid integration. **IEEE Open Access Journal of Power and Energy**, 2024. Available at: <https://doi.org/10.1109/OAJPE.2024.3392246>

SCHRAG, D. P. Confronting the climate–energy challenge. **Elements**, v. 3, p. 171–178, 2007. Available at: <https://doi.org/10.2113/gselements.3.3.171>

SEEBEI, T.; SUNDARAVADIVELU, R. Effect of taut and catenary mooring on spar platform with 5 MW wind turbine. In: **Proceedings of the Eighth ISOPE Ocean Mining Symposium**, Chennai, 2009. Available at: <https://onepetro.org/ISOPEOMS/proceedings-abstract/OMS09/All-OMS09/25385>

TOMASICCHIO, G. R. *et al.* Experimental modelling of the dynamic behaviour of a spar buoy wind turbine. **Renewable Energy**, v. 127, p. 412–432, 2018. Available at: <https://doi.org/10.1016/j.renene.2018.04.061>

UTSUNOMIYA, T. *et al.* Experimental validation for motion of a spar-type floating offshore wind turbine using 1/22.5 scale model. In: **OMAE 2009 - 28th International Conference on Ocean, Offshore and Arctic Engineering**, Honolulu, Hawaii, 2009. Available at: <https://doi.org/10.1115/OMAE2009-79695>

WANG, L.; SWEETMAN, B. Conceptual design of floating wind turbines with large-amplitude motion. In: **SNAME Annual Meeting**, Houston, 2011. Available at: <https://citeseerx.ist.psu.edu/document?repid=rep1&type=pdf&doi=66bd2d662f85d8acfa430c6b52bab5cbeed67ed8>

WIECZOREK, A. J. *et al.* A review of the European offshore wind innovation system. **Renewable and Sustainable Energy Reviews**, v. 26, p. 294–306, 2013. Available at: <https://doi.org/10.1016/j.rser.2013.05.045>

7. ACKNOWLEDGEMENTS

We would like to thank the Fluminense Federal University (UFF) for providing the foundation and support for the development of this work. I also express my gratitude to the Environmental Engineering Program (PEA) at UFRJ and to CAPES for their academic support during the research process. These institutions were fundamental to the completion of this study.